https://doi.org/10.31891/2307-5732-2025-353-6
УДК 681.7, 535.8

BOROVYTSKY VOLODYMYR
National technical university of Ukraine "Igor Sikorsky Kyiv Polytechnic Institute "
https://orcid.org/0000-0001-6816-0391
e-mail: vborovytsky@yahoo.com
AVDIEIONOK IRYNA
National technical university of Ukraine "Igor Sikorsky Kyiv Polytechnic Institute"
https://orcid.org/0009-0007-4709-0030
e-mail: avdeionok.ira@gmail.com

DESIGN OF PHOTONIC INTEGRATED CIRCUITS FOR ANALOG MATRIX TO VECTOR MULTIPLICATION

The article presents a novel and efficient architecture for a photonic integrated circuit (PIC) that performs matrix-vector multiplication using light-based signal processing. This approach leverages the inherent parallelism and ultra-fast propagation speed of photonic systems to execute mathematical operations with unprecedented speed and energy efficiency. The proposed PIC design comprises three functional layers: an input layer, a computational layer, and an output layer.

In the input layer, a predefined array of optical waveguides delivers the incoming optical signals representing the vector to be multiplied. These signals propagate toward the second layer, where the computation occurs. The core innovation lies in the computational layer, which features a matrix of optical apertures. Each aperture has a specific area that is proportional to a corresponding coefficient in the matrix. As light passes through these apertures, its intensity is modulated in a way that naturally implements analog multiplication. This physical encoding allows the optical signals to be multiplied by matrix elements without the need for digital electronics or intermediate conversions.

The third layer contains a second set of optical waveguides that collect the modulated light and direct it to the output, where the result of the matrix-vector multiplication is formed. This design allows real-time analog computations at the speed of light, significantly outperforming conventional electronic processors in both speed and energy efficiency.

A key advantage of this system is its manufacturability. Unlike many photonic systems that require complex and costly photolithographic techniques, this architecture can be fabricated using simpler, low-cost methods, making it accessible for large-scale deployment and integration into current and future optical computing platforms.

The paper introduces a mathematical model and software tools for automatic layout generation, enabling rapid prototyping and customization of the photonic circuits for different computational tasks. Use cases include the implementation of Gaussian filters for signal processing, discrete cosine transforms for data compression, and Hopfield neural networks for memory and pattern recognition tasks.

Moreover, the article provides a comprehensive analysis of the proposed design, evaluating its benefits such as scalability, speed, and energy savings, alongside limitations like precision control and integration challenges. The proposed architecture demonstrates strong potential for applications in neuromorphic computing, real-time data processing, and future photonic AI accelerators.

***Keywords**: photonic integrated circuit, matrix to vector multiplication, automatic layout generation, signal processing, optical waveguide, neural network.*

АВДЄЙОНОК ІРИНА, БОРОВИЦЬКИЙ ВОЛОДИМИР
Національний технічний університет України «Київський політехнічний університет імені Ігоря Сікорського»

ПРОЕКТУВАННЯ ФОТОННИХ ІНТЕГРАЛЬНИХ СХЕМ ДЛЯ АНАЛОГОВОГО МНОЖЕННЯ МАТРИЦІ НА ВЕКТОР

У статті запропоновано нову конструкцію фотонної інтегральної схеми для оптичного множення матриці на вектор. Ця схема містить три шари: перший шар має заданий набір оптичних хвилеводів для вхідних оптичних сигналів, другий шар містить матрицю апертур у якій площі апертур пропорційні коефіцієнтам матриці, третій шар має заданий набір оптичних хвилеводів для вихідних оптичних сигналів. Ця конструкція гарантує аналогове множення зі швидкістю світла, а цю фотонну інтегральну схему можна виготовити без дорогого літографічного обладнання. Представлено математичний апарат для автоматичної генерації топології схеми, його застосування при розробки фотонних інтегральних схем для гаусоввської фільтрації, виконання косинусного перетворення та апаратних реалізацій нейронних мереж Хопфілда та аналіз переваг і недоліків запропонованої конструкції.

У статті представлено нову та ефективну архітектуру фотонного інтегрованого чипа (ФІЧ), що виконує множення матриці на вектор за допомогою оптичної обробки сигналів. Цей підхід використовує природну паралельність та надвисоку швидкість поширення світла, щоб реалізувати математичні операції з безпрецедентною швидкістю та енергоефективністю. Запропонована конструкція ФІЧ складається з трьох функціональних шарів: вхідного, обчислювального та вихідного.

На першому, вхідному, шарі масив оптичних хвилеводів передає вхідні оптичні сигнали, які репрезентують вектор, що множиться. Ці сигнали надходять до другого шару, де виконується основне обчислення. Ключова інновація полягає в обчислювальному шарі, що містить матрицю оптичних апертур. Кожна апертура має площу, пропорційну відповідному коефіцієнту матриці. Під час проходження світла через ці апертури його інтенсивність модулюється, тим самим реалізуючи аналогове множення. Така фізична реалізація дозволяє уникнути необхідності цифрової електроніки чи проміжного перетворення сигналів.

Третій шар містить другий набір оптичних хвилеводів, які збирають модульоване світло та передають його до виходу, де формується результат множення матриці на вектор. Завдяки цій архітектурі обчислення відбуваються в режимі реального часу на швидкості світла, значно перевершуючи традиційні електронні процесори як за швидкістю, так і за енергоспоживанням.

Однією з ключових переваг є простота виготовлення пристрою. На відміну від багатьох фотонних систем, які потребують складних і дорогих фотолітографічних процесів, запропонована архітектура може бути реалізована з використанням доступних, недорогих технологій. Це відкриває шлях до масового виробництва та широкого впровадження у сучасні й майбутні фотонні обчислювальні платформи.

У статті представлено математичну модель та програмні засоби для автоматичної генерації топології, що дає змогу швидко створювати прототипи та адаптувати схеми для різних обчислювальних задач. Застосування охоплює побудову фотонних схем для гаусових фільтрів, дискретного косинус-перетворення та нейронних мереж Хопфілда для реалізації асоціативної пам'яті та розпізнавання образів.

Крім того, подано ґрунтовний аналіз переваг запропонованої конструкції, таких як масштабованість, швидкодія та енергозбереження, а також обговорено можливі обмеження, зокрема точність модуляції та інтеграційні виклики. Архітектура демонструє високий потенціал для застосування в нейроморфних обчисленнях, обробці даних у реальному часі та створенні фотонних прискорювачів штучного інтелекту.

Ключові слова: *фотонна інтегральна схема, множення матриці на вектор, автоматична генерація макета, обробка сигналу, оптичний хвилевід, нейронна мережа.*

Стаття надійшла до редакції / Received 18.04.2025
Прийнята до друку / Accepted 06.05.2025

Introduction

Photonic integrated circuits (PIC) are considered promising devices for telecommunications, signal and image processing, mathematical calculations, hardware implementation of neural networks, deep learning, etc [1]. Matrix to vector multiplication (MVM) remains one of the important operation in these fields of PIC applications. The principal advantage of PICs in comparison with "electronic" integrated circuits is the possibility to perform signal manipulations with s speed of light [1, 2]. That is why PICs are considered as novel accelerators of photonic neural networks or as optical tensor processors [3]. Quantum effects on photonic chips can be also used to perform quantum calculations [4, 5]. Programmable photonic PIC can be built using structures with 2 × 2 blocks, or "analog gates"—the crystal-embedded equivalent of free-space optical splitters based on Mach-Zehnder interferometers (MZIs) [4]. In most cases PICs are implemented by three optical techniques. The first one is based on micro ring resonators (MRRs) as wavelength filters [6 - 8]. Generally, MVM is performed using matrix of MRRs where each MRR act as a selective filter of a definite wavelength [9]. The entire architecture is based on wavelength division multiplexing and a reconfigurable MRRA, which forms a complete 4×4 matrix transmission network. Each MRR can be controlled using a miniature electric heater – temperature variation allows changing MRR spectral transmittance. PICs with MRR for MVM are presented in [10-12]. The alternative PICs uses matrix of MZI for MVM [11-15]. Such PICs based on phase shifting in MZIs to change their transmittance. By application of this technique, PICs can perform positive real value matrix calculation, optical routing, and even optical neural network realization. There are known PICs with a matrix of miniature optical components that can change their transmittance under electrical current [16]. The interesting solution for analog MVM is enLight256 that is able to perform analog MVM with a speed using a 256 x 256 matrix and vector of 256 elements [17,18]. This PIC has a three-layer structure with an expensive spatial light modulator that sufficiently limited its market perspectives. Summarizing said above, it has point out that sophisticated MVM PICs design and expensive technology necessary for their production still remain the principal limitation of wide application of such PICs.

Goal and tasks

The goal is to identify the design procedure for the economical analog PIC for MVM that can be manufactured in the Ukraine without exploitation of expensive equipment likes optical, laser or electron beam lithography. This PIC must be applicable for signal processing, image processing, neural network realizations, automatization and fast mathematical calculations. The following tasks must be solved to reach the goal: identification of PIC structure, creation the mathematical description of PIC layout and development of the algorithms for automatic PIC layout generation.

Methods

The proposed PIC for MVM has three layers structure [19]. The first layer directs optical signals to the aperture matrix. Input optical signals are propagated through a set of optical waveguides and each optical signal enters the second layer. The second layer contains the aperture mask that realizes MVM of input optical signals and the matrix of weight coefficients. The aperture mask contains apertures in a non-transparent film. Aperture diameters proportional to weight coefficients. The result of MVM accumulated by the third layer with a set of optical waveguides for the output optical signals. To ensure maximal possible uniformity of brightness along the waveguides of the first layer, these waveguides are illuminated from both sides (Fig.1). To ensure capturing the output optical signals and the waveguides of the third layers have detectors of optical radiation on both sides as well (Fig. 1). To ensure integration and averaging of optical radiation via multiple diffusive reflections all optical waveguides have the shape of a parallelepiped made of transparent plastics and, their side idle faces have diffused reflective surfaces.

Generally, the input signals and the weight coefficients can be positive and negative. That is why the proposed PIC should guarantee MVM considering the signs of input signals and the weight coefficients. The following PIC topology can realize such MVM.

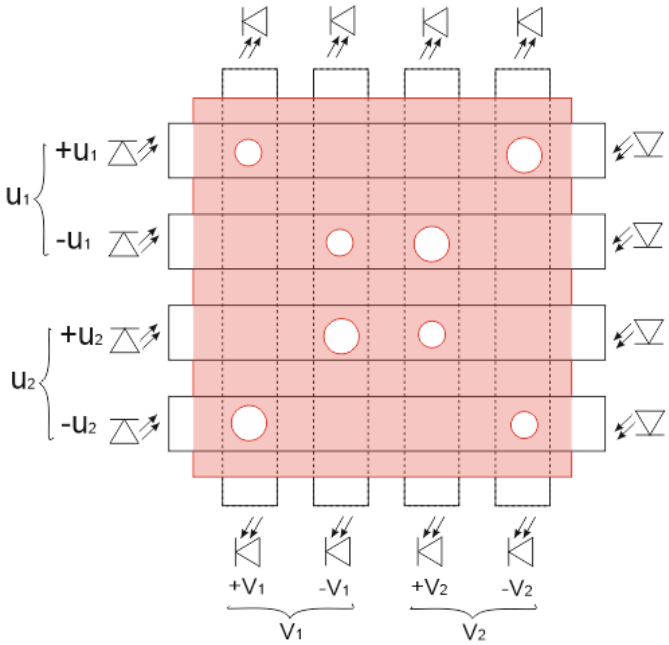

Fig.1 Topology of the proposed PIC

At the beginning the input data has to be specified: number of input optical signals N_Y, number of output optical signals N_X, the matrix of the weight coefficients $M_{ky, kx}$ and limitations to the linear dimensions of the PIC working area X_W,Y_W. The topology of the proposed PIC has the separate waveguides for positive and negative values of input and output optical signals. In the case of MVM with 2 x 2 matrix the waveguides for input optical signals are u_1 and u_2, and the waveguides for output optical signals output channels are v_1 i v_2 (Fig. 1).

To perform formation of optical signals from both sides of the waveguides and capture output optical signals from both sides of the waveguide the economical electrical schemes can be applied (Fig. 2, 3). The scheme with Schmitt triggers forms binary output electrical signals that are necessary for hardware realization of optical neural networks (Fig. 2). The scheme with differential amplifiers helps to realize fast analog MVM using positive and negative values (Fig.3).

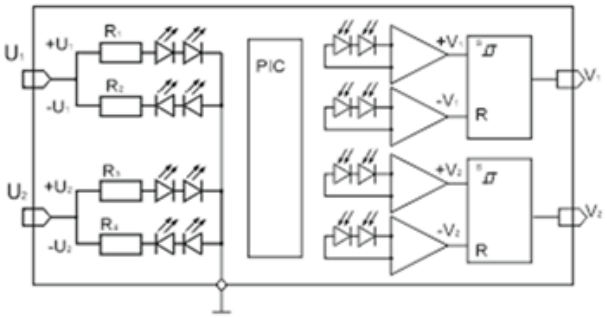

Fig.2 PIC for realization of the optical neural network

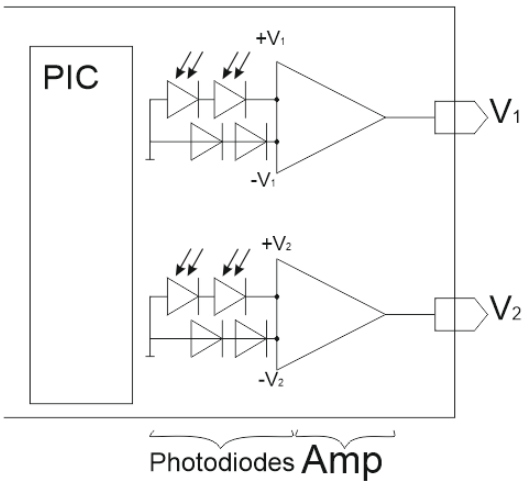

Fig. 3 PIC for realization of fast analog MVM

Let us go to mathematical description of PIC layout. This layout contains a two-dimensional structure of cells for positive and negative components of each input and output signal (Fig. 4). The first and the third layers have the set of the optical waveguides that connect these cells in the perpendicular direction (Fig. 2). The second layer has the matrix of circular apertures of different diameters. At the beginning it has to calculate the coordinates of the centers of these cells:

$$cx_{kx} = \Delta x \cdot (0.5 + k_X - 1) \quad (1)$$
$$cy_{kx} = \Delta y \cdot (0.5 + k_Y - 1)$$

where k_Y, k_X – the indexes of the input optical waveguide in the first layer and the number of the output optical waveguide in the third layer - $k_X = [\,0 \ldots N_X - 1\,]$, $k_Y = [\,0 \ldots N_Y - 1\,]$, respectively; N_Y, N_X – the number of the input optical waveguide in the first layer and the number of the output optical waveguide in the third layer, respectively; Δx, Δy – the spatial periods of the cells along coordinate axes X and Y, respectively: $\Delta x = X_W/N_X$, $\Delta y = Y_W/N_Y$; X_W, Y_W – the dimensions of the PIC working area along axes X and Y respectively; cx_{kx}, cy_{ky} – the coordinates of the center of cell (k_X, k_Y), respectively.

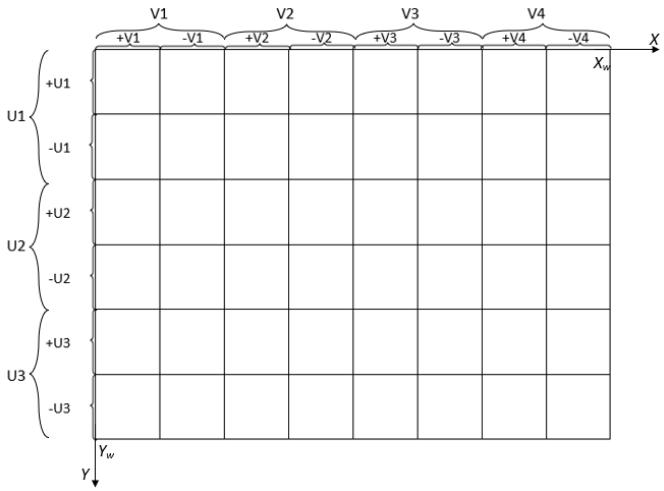

Fig.4 Coordinate system of PIC layers

Each cell has two inputs: the first is for positive input values and the second is for negative ones (Fig. 4, 5). It has also two outputs: the first is for positive output values and the second is for negative ones. To realize analog multiplication two similar apertures for each cell are necessary. These two apertures link the positive and negative input signals with positive and negative output signals depending on the sign of the weight coefficient. The coordinates of aperture centers are linked to the cell centers (1):

$$ax1_{kx} = cx_{kx} + 0.25 \cdot s_{ky,kx} \cdot \Delta x \quad ay1_{kx} = cy_{ky} - 0.25 \cdot s_{ky,kx} \cdot \Delta y \quad (2)$$
$$ax2_{kx} = cx_{kx} - 0.25 \cdot s_{ky,kx} \cdot \Delta x \quad ay2_{kx} = cy_{ky} + 0.25 \cdot s_{ky,kx} \cdot \Delta y$$

Where, $ax1_{kx}$, $ay1_{ky}$, $ax2_{kx}$, $ay2_{ky}$ – the coordinates of the center of two apertures (k_X, k_Y) located in one cell, respectively; $s_{ky,kx}$ – the value that specifies the sign of the weight coefficient $M_{ky,kx}$: if $M_{ky,kx} > 0$ then $s_{ky,kx} = 1$ otherwise $s_{ky,kx} = -1$.

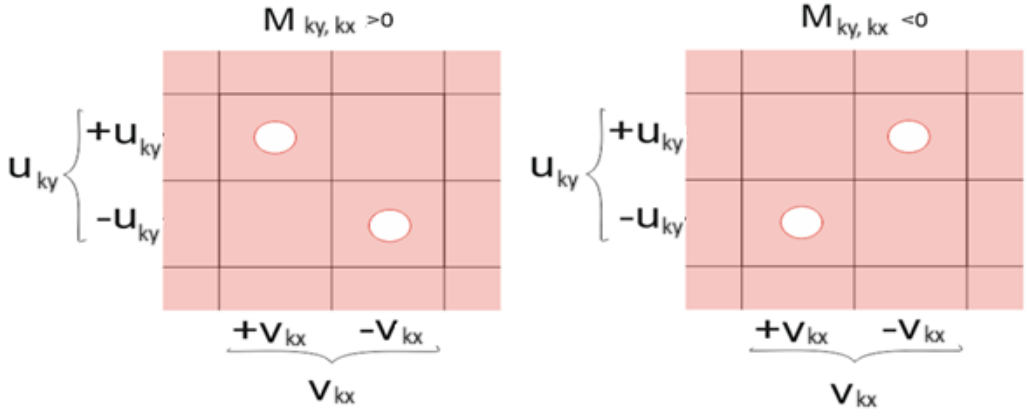

Fig.5 PIC cell that performs analog multiplication

The area of each pair of apertures is proportional to the corresponding weight coefficient. It has to normalize aperture dimensions relatively the maximal possible weight coefficient value and the maximal possible aperture area [20]. It is also necessary to consider the losses in the input and output waveguides:

$$C_{ky,kx} = W1_{ky} \cdot W2_{kx} \cdot M_{ky,kx} \quad (3)$$

where $C_{ky,kx}$ – the matrix of weight coefficients after corrections of the losses of optical radiation in input and output optical waveguides;

$W1_{ky}$, $W2_{kx}$ – the coefficients for correction of the losses of optical radiation in input and output waveguides, respectively. These losses can be approximated by exponential functions [20]:

$$W1_{ky} = \frac{1}{L_Y(ay_{ky})} = \frac{1}{\frac{2b+(1-b)\cdot\left(\exp\left(-k\cdot\frac{ay_{ky}}{Y_w}\right)+\exp\left(-k\left(1-\frac{ay_{ky}}{Y_w}\right)\right)\right)}{1+b+\exp(-k)}} = \frac{1+b+\exp(-k)}{2b+(1-b)\cdot\left(\exp\left(-k\cdot\frac{ay_{ky}}{Y_w}\right)+\exp\left(-k\cdot\left(1-\frac{ay_{ky}}{Y_w}\right)\right)\right)}$$

$$W2_{kx} = \frac{1}{L_Y(ax_{kx})} = \frac{1}{\frac{2b+(1-b)\cdot\left(\exp\left(-k\cdot\frac{ax_{kx}}{Y_w}\right)+\exp\left(-k\cdot\left(1-\frac{ax_{kx}}{X_w}\right)\right)\right)}{1+b+\exp(-k)}} = \frac{1+b+\exp(-k)}{2b+(1-b)\cdot\left(\exp\left(-k\cdot\frac{ax_{kx}}{X_w}\right)+\exp\left(-k\cdot\left(1-\frac{ax_{kx}}{X_w}\right)\right)\right)}$$

Ly(y) – the losses coefficient of optical flux in the input waveguide as the function of aperture center x. The experimental research confirmed that this distribution can be described using exponential functions [20]:

$$L_Y(y) = \frac{2b+(1-b)\cdot\left(\exp\left(-k\cdot\frac{y}{Y_w}\right)+\exp\left(-k\left(1-\frac{y}{Y_w}\right)\right)\right)}{1+b+\exp(-k)}$$

Lx(x) – the losses coefficient of optical flux in the output waveguide as the function of aperture center *y* .

$$L_X(x) = \frac{2b+(1-b)\cdot\left(\exp\left(-k\cdot\frac{x}{X_w}\right)+\exp\left(-k\cdot\left(1-\frac{x}{X_w}\right)\right)\right)}{1+b+\exp(-k)}$$

k, b – the coefficients that depends on waveguide material and design, they can be measured experimentally [20].

Now it is possible to calculate the dimensions of each aperture in the second layer. The following assumptions help to simplify the PIC layout:

- all apertures have the shape of an ellipse;
- the maximal aperture dimensions along axis's X and Y (sx, sy) are equal to width of the corresponding input and output waveguides: sx < 0.5· Δx and sy < 0.5·Δy;
- the area of the apertures is proportional to the matrix of weight coefficients after corrections $C_{ky,kx}$ (3).

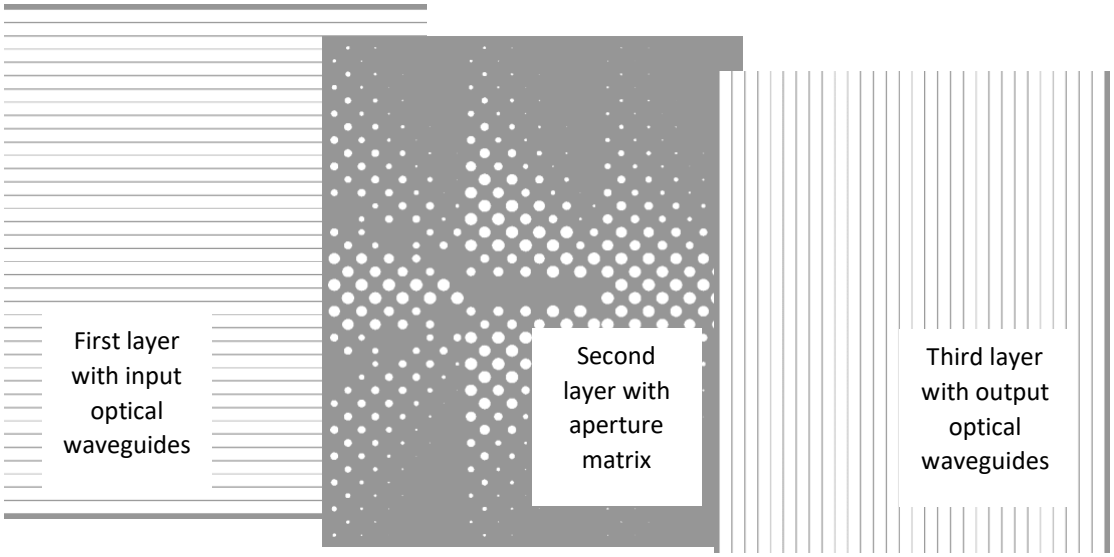

Fig 6. Layout of three-layer PIC for analog MVM

As a result, the aperture dimensions can be calculated using the following expressions:

$$asy_{ky,kx} = 2 \cdot ex_{ky,kx} = 2 \cdot \sqrt{\frac{A_{ky,kx}}{\pi} \cdot \frac{sx}{sy}} \tag{4}$$

$$asx_{ky,kx} = 2 \cdot ey_{ky,kx} = 2 \cdot e_{ky,kx} \cdot \frac{sy}{sx}$$

$$A_{ky,kx} = \pi \cdot ex_{ky,kx} \cdot ey_{ky,kx} = \frac{|C_{ky,kx}|}{C_{max}} \cdot A_{max} = \frac{|C_{ky,kx}|}{C_{max}} \cdot (\pi \cdot sx \cdot sy)$$

where $asx_{kx,ky}$, $asy_{kx,ky}$, $ex_{kx,ky}$, $ey_{kx,ky}$ – the dimensions and the semi axis's of the aperture in the cell *(kx, ky)* along axis's X and Y, respectively; $A_{kx,ky}$ – the area of the aperture in the cell *(kx, ky)* along axis's X and Y that is proportional to the weight coefficient $C_{kx,ky}$; A_{max}, C_{max} – the maximal values of the aperture area and the absolute value of the weight coefficient $C_{ky,kx}$ – $A_{max} = \pi \cdot sx \cdot sy$, $C_{max} = \max(|C_{ky,kx}|)$ respectively.

The presented mathematical apparatus (1)-(4) allows calculation of geometrical parameters of PIC for MVM and automatic generation the PIC layout for any given matrix of weight coefficients. There has been developed special software that makes all operations necessary for generation of the PIC layout in raster and vector formats (Fig. 6).

Table 1

PIC design for Gaussian filtration.

№	Filter impulse response	Parameter, σ
1	Gaussian function	1.0
2		1.5
3		2.0
4		2.5
5		3.0
6	First derivative of Gaussian function	1.0
7		1.5
8		2.0
9		2.5
10		3.0
11	Second derivative of Gaussian function	1.0
12		1.5
13		2.0
14		2.5
15		3.0

Table 2

Four symbols 4 x 8 used for calculation of the coefficients of Hopfield neural network

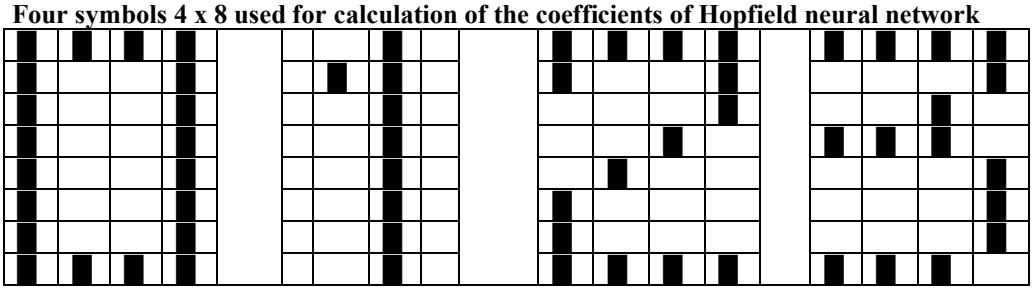

Results

The proposed technique (1)-(4) is used for automatic generation of three PIC layouts. The first design is PIC that performs Gaussian filtration of input optical signals coming from 19 input optical waveguides. This PIC produces output signals of 15 linear filters at the same time for one input signal (Table 1, Pic. 7a).

The second PIC design is for a cosine-transform, which is used in JPEG compression (Fig. 7, b). This PIC has 16 input signals, and it can calculate 16 coefficients of cosine-transform in the same time.

The third PIC design is for hardware realization of Hopfield networks (Fig. 7c). Its aperture mask contains the coefficients of Hopfield network that is prepared for recognition of four symbols 0, 1, 2 and 3 that are represented using 4 x 8 matrix of binary values (Table 2). All the PIC designs can be scaled to the given dimensions (X_W, Y_W) and the given number of input and output waveguides (Nx, Ny).

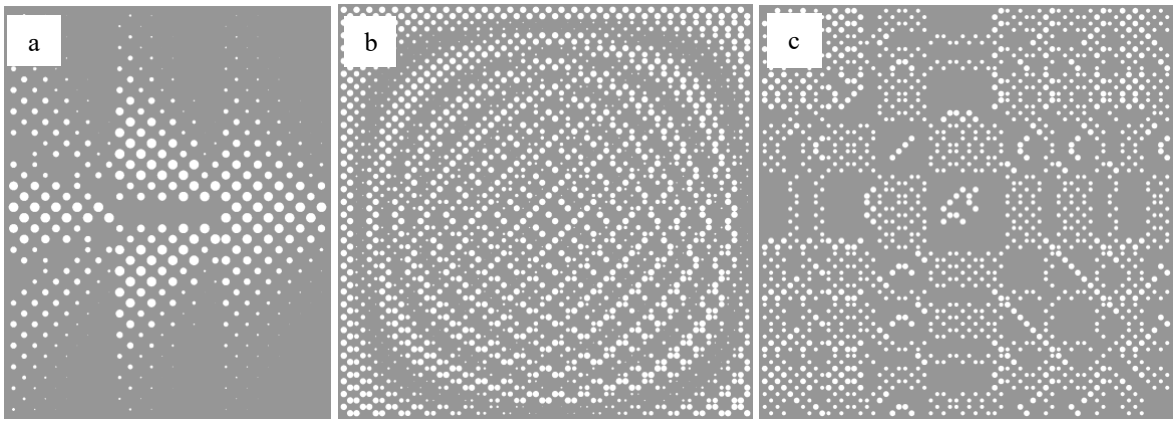

Fig 7. Three PIC designs: a) PIC for Gaussian filtration; b) PIC for cosine-transform, c) PIC for Hopfield network

Discussion

The proposed PIC design has the following advantages:

- It performs very fast analog MVM that is limited only be switching input signals and reading out the output ones;
- Potentially it can do MVM on multiple wavelengths in one PIC;
- Its optical part is not sensitive to high frequency electromagnetic signal and fields;

- The principal advantage is the economical design – only set of plastic waveguides, one non-transparent film with apertures, plastic housing and a set of light emitted diodes and photodiodes are necessary for serial manufacture of these PICs, no expensive equipment (laser, optical, e-beam lithography) necessary for mass production (Fig. 8) [21];
- The design procedure (1)-(4) can be easy automatized by the computer aid design software that generate all layouts for given requirements.

The disadvantages of the PIC design for analog optical MVM include:

- Fixed second layer with aperture matrix that make impossible changing the weight coefficients during the PIC operation, on the contrary in the PICs with MZI or MRR matrixes these coefficients can be changed in any time using electrical signals;
- PIC dimensions are of cm range. It is a result of economical technological process based on plastic waveguide cutting and polishing and aperture matrix made from aluminum foil by laser graving [21];
- The dimensions of PICs are proportional to the number of input and output signals. Assembling the PICs when the number of waveguides exceeds 30 becomes complicated and the dimensions of such PIC may overcome 15 cm that is not convenient for embedded system. Also, in long optical waveguides variance of optical properties decreases accuracy of analog optical MVM. That is why the reasonable number of input and output signals is in the range from 8 to 32.
- The principal disadvantage is the sufficient errors due to analog MVM. This error is caused by variations of light emitted diodes and photodiodes characteristics, variations of waveguide optical characteristics, multiple crosstalk (radiation exchange) between input and output waveguides and other factors. These errors can be partly compensated but, in any case, the total error remains in a range of 5 – 10 %. Application of binary aperture masks when the weight coefficients are equal to -1 or 1 can minimize the total due to usage of apertures with maximal possible area.

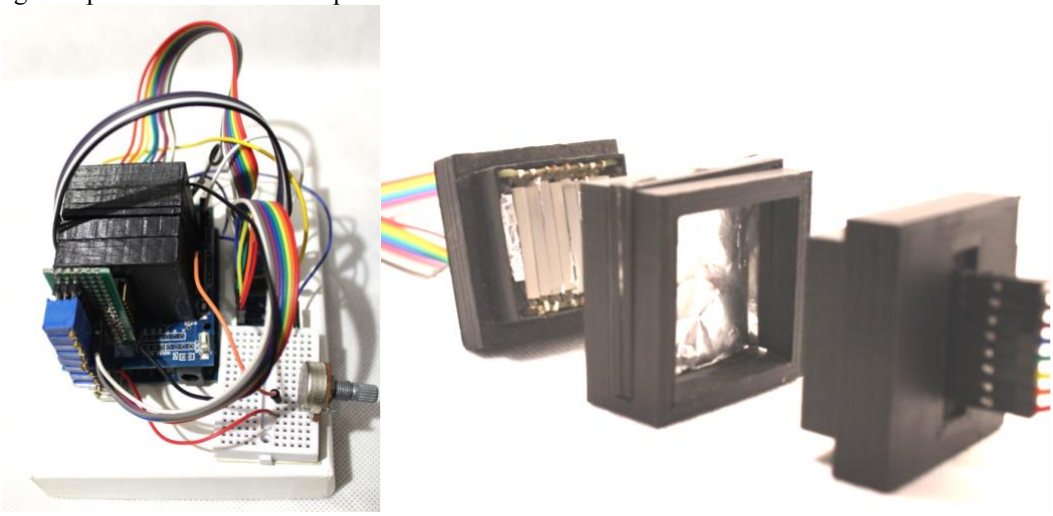

Fig 8. Assembled (on the left) and disassembled (on the right) prototype of three-layer MVM PIC

Conclusion

The proposed design procedure makes possible automatic layout generation for the economical three-layer PIC for analog optical MVM. This procedure allows calculation of geometry of waveguides and aperture matrix that guarantees multiplication of the input signal to the given matrix of weight coefficients. The procedure is based on the mathematical model which helps to calculate dimensions and coordinates of the apertures necessary for multiplication of positive and negative values. PIC layout is generated in raster and vector formats that can be used by laser cutting and laser graving tools. Manufacture of the proposed PIC does not require expensive equipment like electron, laser or optical lithography of micrometer scale.

These PICs have perspectives in fast hardware realization of neural networks with small number of neurons (up to 16 - 32), fast signal processing and fast analog MVM with small number of inputs (up to 16 - 32).

The proposed PICs are useful in optical education because their design, manufacture, testing and evaluation improve student knowledge of mathematics and physics, software development skills, material processing skills, electronic measurement skills and, as a result, it stimulates interest to optical engineering and photonics, including perspectives of photonic artificial intelligence [19].

References

1. Bai B., Shu H., Wang X. et al. (2020) Towards silicon photonic neural networks for artificial intelligence. Sci. China Inf. Sci. 63, 160403. https://doi.org/10.1007/s11432-020-2872-3

2. Kennedy P. (2022) Lightmatter Passage brings Co-Packaged Optics and Silicon Photonics to the Chiplet Era. Retrieved from https://www.servethehome.com/lightmatter-passage-brings-co-packaged-optics-and-silicon-photonics-to-the-chiplet-era/

3. Wenyu Chen et al. (2024) Pixelated non-volatile programmable photonic integrated circuits with 20-level intermediate states, International Journal of Extreme Manufacturing 6, 035501. https://doi.org/10.1088/2631-7990/ad2c60

4. Bogaerts, W., Pérez, D., Capmany, J. et al. Programmable photonic circuits. Nature 586, 207–216 (2020). https://doi.org/10.1038/s41586-020-2764-0

5. Luo, W., Cao, L., Shi, Y. et al. (2023) Recent progress in quantum photonic chips for quantum communication and internet. Light Sci Appl 12, 175. https://doi.org/10.1038/s41377-023-01173-8

6. V. Bangari et al. (2020) Digital Electronics and Analog Photonics for Convolutional Neural Networks (DEAP-CNNs). IEEE Journal of Selected Topics in Quantum Electronics, vol. 26, no. 1, pp. 1-13,. https://doi.org/10.1109/JSTQE.2019.2945540

7. Huang C., Bilodeau S., Ferreira de Lima T. et al. (2020) Demonstration of scalable microring weight bank control for large-scale photonic integrated circuits. APL Photonics 1 April 2020; No 5 (4) 040803. https://doi.org/10.1063/1.5144121

8. Ohno S., Toprasertpong K., Takagi S., Takenaka M. (2020) Si microring resonator crossbar arrays for deep learning accelerator, Japanese Journal of Applied Physics, Vol. 59, No. SG. https://doi.org/10.35848/1347-4065/ab6d82

9. Cheng J, Zhou H, Dong J. (2021) Photonic Matrix Computing: From Fundamentals to Applications. Nanomaterials, No 11(7):1683. https://doi.org/10.3390/nano11071683

10. Huang C., Bilodeau S., Ferreira de Lima T. et al. (2020) Demonstration of scalable microring weight bank control for large-scale photonic integrated circuits. APL Photonics, No 5(4) 040803. https://doi.org/10.1063/1.5144121

11. Zhou, H., Dong, J., Cheng, J. et al. (2022) Photonic matrix multiplication lights up photonic accelerator and beyond. Light: Science & Applications, Vol. 11, No 30. https://doi.org/10.1038/s41377-022-00717-8

12. Cheng, J., Zhao, Y., Zhang, W. et al. (2022) A small microring array that performs large complex-valued matrix-vector multiplication. Frontiers of Optoelectronics, 15, 15. https://doi.org/10.1007/s12200-022-00009-4

13. Zhou H., Zhao Y., Wang X. et al. (2021) Self-configuring and reconfigurable silicon photonic signal processor, ACS Photonics, No 7(3), p. 792-799. https://doi.org/10.1021/acsphotonics.9b01673

14. Torrijos-Morán L., Pérez-Galacho D., Pérez-López D. (2024) Silicon Programmable Photonic Circuits Based on Periodic Bimodal Waveguides. Laser Photonics Rev, No18, p.2300505. https://doi.org/10.1002/lpor.202300505

15. Carolan J.J., Prabhu M, Skirlo S.A., Shen Y., Soljacic M., Englund D., Harris N.C. (2022) Apparatus and methods for optical neural network, U.S. patent number 11,334,107 B2, issued in May 2022. Retrieved from https://patents.google.com/patent/US10268232B2/en

16. Cheng J, Zhou H, Dong J. (2021) Photonic Matrix Computing: From Fundamentals to Applications. Nanomaterials, No 11(7):1683. https://doi.org/10.3390/nano11071683

17. Neena Barhen J. (2009) Acoustic Source Localization via Time Difference of Arrival Estimation for Distributed Sensor Networks Using Tera-Scale Optical Core Devices. Journal of Sensors. 1-12. https://doi.org/10.1155/2009/187916

18. Borovytsky V., Avdeieionok I., Tuzhanskyi S., Lysenko H. (2022) Photonic integrated circuits for optical matrix-vector multiplication. Optoelectronic Information-Power Technologies, Vol.43, No 1, p. 11–18. https://doi.org/10.31649/1681-7893-2022-43-1-11-18

19. Borovytsky V., Avdeieionok I. (2024) Economical optical matrix to vector multiplier. Proc. SPIE 12938, 129381F. https://doi.org/10.1117/12.3013064

20. Avdeieionok I., Borovytsky V. (2024) Characterisation of optical waveguides for photonic integrated circuits Bulletin of Cherkasy State Technological University, Vol. 29, No. 2, p. 24-31. https://doi.org/10.62660/bcstu/2.2024.24

21. Avdeieionok I., Borovytsky V. (2024) Photonic Integrated Circuit and its calibration. Herald of Khmelnytskyi National University. Technical Sciences, No 331(1), p. 11-17. https://doi.org/10.31891/2307-5732-2023-331-1

Література

1. Bai B., Shu H., Wang X. et al. (2020) Towards silicon photonic neural networks for artificial intelligence. Sci. China Inf. Sci. 63, 160403. https://doi.org/10.1007/s11432-020-2872-3

2. Kennedy P. (2022) Lightmatter Passage brings Co-Packaged Optics and Silicon Photonics to the Chiplet Era. Retrieved from https://www.servethehome.com/lightmatter-passage-brings-co-packaged-optics-and-silicon-photonics-to-the-chiplet-era/

3. Wenyu Chen et al. (2024) Pixelated non-volatile programmable photonic integrated circuits with 20-level intermediate states, International Journal of Extreme Manufacturing 6, 035501. https://doi.org/10.1088/2631-7990/ad2c60

4. Bogaerts, W., Pérez, D., Capmany, J. et al. Programmable photonic circuits. Nature 586, 207–216 (2020). https://doi.org/10.1038/s41586-020-2764-0

5. Luo, W., Cao, L., Shi, Y. et al. (2023) Recent progress in quantum photonic chips for quantum communication and internet. Light Sci Appl 12, 175. https://doi.org/10.1038/s41377-023-01173-8

6. V. Bangari et al. (2020) Digital Electronics and Analog Photonics for Convolutional Neural Networks (DEAP-CNNs). IEEE Journal of Selected Topics in Quantum Electronics, vol. 26, no. 1, pp. 1-13,. https://doi.org/10.1109/JSTQE.2019.2945540

7. Huang C., Bilodeau S., Ferreira de Lima T. et al. (2020) Demonstration of scalable microring weight bank control for large-scale photonic integrated circuits. APL Photonics 1 April 2020; No 5 (4) 040803. https://doi.org/10.1063/1.5144121

8. Ohno S., Toprasertpong K., Takagi S., Takenaka M. (2020) Si microring resonator crossbar arrays for deep learning accelerator, Japanese Journal of Applied Physics, Vol. 59, No. SG. https://doi.org/10.35848/1347-4065/ab6d82

9. Cheng J, Zhou H, Dong J. (2021) Photonic Matrix Computing: From Fundamentals to Applications. Nanomaterials, No 11(7):1683. https://doi.org/10.3390/nano11071683

10. Huang C., Bilodeau S., Ferreira de Lima T. et al. (2020) Demonstration of scalable microring weight bank control for large-scale photonic integrated circuits. APL Photonics, No 5(4) 040803. https://doi.org/10.1063/1.5144121

11. Zhou, H., Dong, J., Cheng, J. et al. (2022) Photonic matrix multiplication lights up photonic accelerator and beyond. Light: Science & Applications, Vol. 11, No 30. https://doi.org/10.1038/s41377-022-00717-8

12. Cheng, J., Zhao, Y., Zhang, W. et al. (2022) A small microring array that performs large complex-valued matrix-vector multiplication. Frontiers of Optoelectronics, 15, 15. https://doi.org/10.1007/s12200-022-00009-4

13. Zhou H., Zhao Y., Wang X. et al. (2021) Self-configuring and reconfigurable silicon photonic signal processor, ACS Photonics, No 7(3), p. 792-799. https://doi.org/10.1021/acsphotonics.9b01673

14. Torrijos-Morán L., Pérez-Galacho D., Pérez-López D. (2024) Silicon Programmable Photonic Circuits Based on Periodic Bimodal Waveguides. Laser Photonics Rev, No18, p.2300505. https://doi.org/10.1002/lpor.202300505

15. Carolan J.J., Prabhu M, Skirlo S.A., Shen Y., Soljacic M., Englund D., Harris N.C. (2022) Apparatus and methods for optical neural network, U.S. patent number 11,334,107 B2, issued in May 2022. Retrieved from https://patents.google.com/patent/US10268232B2/en

16. Cheng J, Zhou H, Dong J. (2021) Photonic Matrix Computing: From Fundamentals to Applications. Nanomaterials, No 11(7):1683. https://doi.org/10.3390/nano11071683

17. Neena Barhen J. (2009) Acoustic Source Localization via Time Difference of Arrival Estimation for Distributed Sensor Networks Using Tera-Scale Optical Core Devices. Journal of Sensors. 1-12. https://doi.org/10.1155/2009/187916

18. В. Боровицький, І. Авдєйонок, С. Тужанський, і Г. Лисенко (2022) «Фотонні інтегральні схеми для оптичного матриць-векторного множення», Опт-ел. інф-енерг. техн., вип. 43, вип. 1, с. 11–18. https://doi.org/10.31649/1681-7893-2022-43-1-11-18

19. Borovytsky V., Avdeieionok I. (2024) Economical optical matrix to vector multiplier. Proc. SPIE 12938, 129381F. https://doi.org/10.1117/12.3013064

20. Авдєйонок І., Боровицький В. (2024) Характеристика оптичних хвилеводів для фотонних інтегральних схем, Вісник Черкаського державного технологічного університету, Том 29, № 2, с. 24-31. https://doi.org/10.62660/bcstu/2.2024.24

21. Авдєйонок, І., Боровицький, В. (2024). Фотонна інтегральна схема та її калібрування. Вісник Хмельницького національного університету. Серія: Технічні науки, Том 331, № 1, с. 11-17. https://doi.org/10.31891/2307-5732-2023-331-1